Cognition 212 (2021) 104709

Contents lists available at ScienceDirect

Cognition

journal homepage: www.elsevier.com/locate/cognit

Serial dependence does not originate from low-level visual processing

Gizay Ceylan *, Michael H. Herzog, David Pascucci

Laboratory of Psychophysics, Brain Mind Institute, École Polytechnique Fédérale de Lausanne (EPFL), Lausanne, Switzerland

ARTICLE INFO

Keywords:
Serial dependence
History bias
Perception
Decision inertia

ABSTRACT

Perception depends not only on the current sensory input but also on the preceding history of stimuli. In serial dependence (SD), for example, the orientation of a Gabor patch is mistakenly reported as more similar to previous trials than it actually is. This bias is typically observed for moderate orientation differences (<45°) and extends over a few trials in the past. It is hotly debated whether SD originates at perceptual or post-perceptual, e.g., decisional, stages. Here, we provide evidence for the latter hypothesis. We presented Gabor patches with different spatial frequencies or Gabors intermingled with dot patterns. Even though stimuli were perceptually clearly dissimilar, we found robust SD effects arguing against any perceptual account. These findings suggest a re-evaluation of current models and theoretical accounts of SD.

1. Introduction

We live under the impression of perceiving the world simply as it is. Yet, perception is systematically distorted by all sorts of spatial and temporal contexts, strikingly evident in many illusions. In the temporal domain, studies on *serial dependence* (SD; Fischer & Whitney, 2014) have shown that human perception of a current stimulus is systematically biased toward stimuli presented just before. In a typical SD task, for example, observers adjust the orientation of a Gabor patch in a series of trials (Fig. 1). Even though the interval between consecutive Gabors can be substantially long (e.g., up to 5 s), responses to the present Gabor are systematically biased toward orientations seen a few trials before.

It is widely believed that SD is perceptual (Cicchini, Mikellidou, & Burr, 2017; Fischer & Whitney, 2014; Manassi, Liberman, Kosovicheva, Zhang, & Whitney, 2018) but several works support the involvement of *post-perceptual* processes (i.e., working memory, decision-making; Fritsche, Mostert, & de Lange, 2017; Bliss, Sun, & D'Esposito, 2017; Pascucci et al., 2019). Although simplistic, the perceptual/post-perceptual dichotomy has been widely used in the attempt to elucidate the mechanisms behind SD (Fritsche et al., 2017; Pascucci et al., 2019), particularly in relation to negative forms of serial dependence, like adaptation and aftereffects, which have a clear perceptual nature (Gibson, 1937). A more useful distinction is between the *source* and the *site of action* of SD (Cicchini et al., 2021), i.e., whether SD originates at a perceptual or post-perceptual stage and whether it affects future processing at early or later stages. By this distinction, it is possible to hypothesize, for instance, that SD emerges post-perceptually (late source) and affects early visual processing and stimulus appearance in the next trial (early site).

In the purely perceptual view (source and site of action are related to low level processing), SD is often explained by a so-called *continuity field*, which combines features of similar stimuli within an extended region of space (~15° of visual angle) and time (~10–15 s) into a single percept (Fischer & Whitney, 2014). The underlying idea is that the visual world is relatively stable within short temporal windows and, hence, previous events can be used as priors for the present percept, reducing the effect of external noise and providing stability across eye movements (Cicchini, Mikellidou, & Burr, 2018; van Bergen & Jehee, 2019). Models of SD are thus in the Bayesian and adaptive filtering spirit where prior and current stimuli are combined depending on their relative reliability (Cicchini et al., 2018; Fritsche, Spaak, & de Lange, 2020; van Bergen & Jehee, 2019).

Evidence in support of the post-perceptual view comes from studies showing that SD is driven by post-perceptual aspects, such as working memory and decision-making processes (Fritsche et al., 2017; Pascucci et al., 2019; but see Cicchini et al., 2017), requires conscious and attentional processing (Fritsche & de Lange, 2019; Kim, Burr, Cicchini, & Alais, 2020) and does not occur for behaviorally irrelevant stimuli (Fischer & Whitney, 2014). Accordingly, alternative models have been suggested related to decisional rather than continuity fields (Pascucci et al., 2019).

Here, we tested whether SD originates from low- or high-level processing. We presented Gabor patches with a high and a low spatial frequency (SF) within the same block of trials (Experiment 1) or Gabors intermixed with symmetric dot patterns (Experiment 2). The rationale is

* Corresponding author at: EPFL SV BMI LPSY, SV 2805 (Bâtiment SV) Station 19, CH-1015 Lausanne, Switzerland.
E-mail address: gizay.ceylan@epfl.ch (G. Ceylan).

https://doi.org/10.1016/j.cognition.2021.104709
Received 7 August 2020; Received in revised form 25 March 2021; Accepted 26 March 2021
Available online 7 April 2021

that these stimuli do not only differ in their appearance but also share very limited processing. At the earliest stages of vision, for instance, Gabors with different spatial frequencies are processed by distinct neuronal populations (Georgeson, 1973; Ware & Mitchell, 1974). The orientation of the dot patterns, instead, requires the computation of symmetry, which occurs only for neurons in higher visual areas such as, for instance, the lateral occipital cortex, V4 and V7 (Bertamini, Silvanto, Norcia, Makin, & Wagemans, 2018; Sasaki, Vanduffel, Knutsen, Tyler, & Tootell, 2005; Wang et al., 2016). Hence, if SD occurs only between Gabors of the same SF, our results speak for a perceptual effect. However, if SD occurs between different Gabors or even between Gabors and dot patterns, a purely perceptual account can be ruled out.

2. General methods

2.1. Ethics statement

The study was approved by the local ethics committee in accordance with the Declaration of Helsinki (except for preregistration) (World Medical Organization, 2013).

2.1.1. Apparatus

Stimuli were presented on a gamma-corrected VG248QE monitor (resolution: 1920 × 1080 pixels, refresh rate: 120 Hz) and were generated with custom-made scripts written in Matlab (R2013a) and the Psychophysics Toolbox (Brainard, 1997), running on a Windows-based machine. Experiments were performed in a darkened room, and participants sat at 57 cm from the computer screen, with their head positioned on a chin rest. All stimuli were presented on a grey background (62.66 cd/m^2).

2.2. Participants

A total of 48 healthy participants (two independent groups of 24, age range of 18–40 years, 10 females in Experiment 1 and 11 females in Experiment 2), mostly from the EPFL and the University of Lausanne, participated in the study for a monetary reward (20 CHF/h). All participants had normal or corrected-to-normal vision and were naïve as to the purpose of the experiments. Visual acuity was tested with the Freiburg Acuity test, and a value of 1 had to be reached with both eyes open (Bach, 1996). Written informed consent was collected from all participants in advance. Participants were instructed to maintain their gaze at the centre of the screen for the entire duration of the experiment.

2.2.1. Stimuli and procedures

An example of a trial sequence in Experiment 1 is illustrated in Fig. 1A-B. Each trial started with a green fixation dot (0.5°, 500 ms) followed by a central Gabor lasting 500 ms. Gabor stimuli were Gaussian-windowed sinusoidal gratings with a peak contrast of 25% Michelson and a Gaussian envelope of 1.5°. The spatial frequencies of Gabor stimuli were either 0.33 (Low SF) or 1 (High SF) cycle(s) per degree. After the Gabor, a noise mask was presented, centred at the same location for 500 ms. Masks were white-noise patches of the same size of the Gabor stimuli with a peak contrast of 95% Michelson, smoothed with a symmetric Gaussian low-pass filter (filter size = 1°, SD = 2°). After a blank fixation interval of 500 ms, a response tool was presented at the same location as the Gabor. The response tool was a dark grey circular frame surrounding the location of the previous Gabor with two symmetric dots (0.5° of diameter) that marked the extremities of an imaginary oriented line. This response tool was designed to reduce the effect of additional physical orientation signals in stimulus-related serial

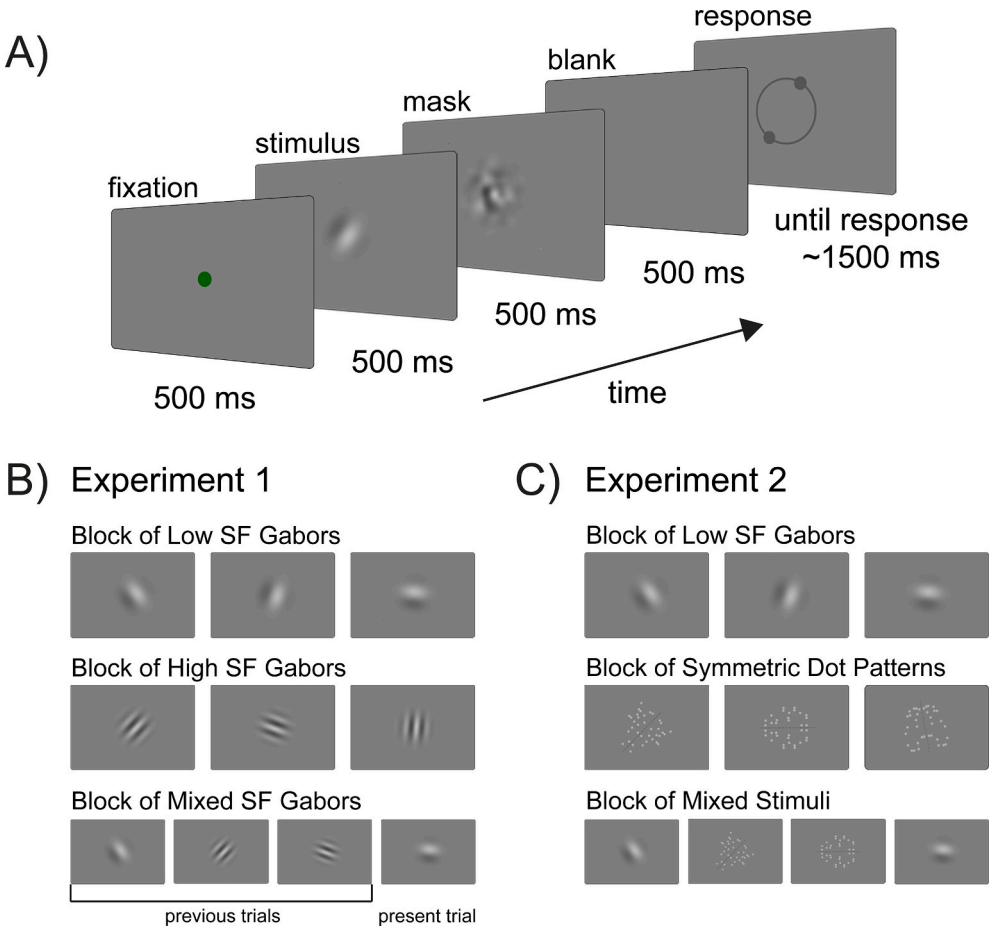

Fig. 1. A) Example of a trial sequence in the orientation adjustment task. Participants saw an oriented Gabor stimulus at the centre of the screen, followed by a noise mask. After a blank interval, participants reported the orientation of the stimulus by adjusting the angle of an imaginary line connecting two dots connected by a thin circle. B) In Experiment 1, separate blocks contained Gabors with low (Low SF; 0.33 cpd), high (High SF; 1 cpd), or mixed (Mixed SF) spatial frequencies. In the mixed block, Gabors of low and high spatial frequencies were randomly interleaved. C) In Experiment 2, High SF Gabors were replaced by patterns of symmetric dots, and participants reproduced the tilt based on the angle of the symmetry axis. The symmetry axis is indicated by the dashed black lines (not presented in the experiment). The order of blocks was counterbalanced across participants. Stimuli are not drawn to scale.

dependence. On each trial, the orientation of the response tool was set randomly, and participants were asked to adjust it until it matched the perceived orientation of the Gabor. The response tool was rotated by moving the computer mouse in the upward (clockwise rotation) or downward (counterclockwise rotation) directions, and the final response was confirmed by pressing the keyboard space bar. After a random intertrial interval (500–1000 ms), a new trial started. Gabor stimuli were assigned random orientations in each trial, covering the entire orientation range (0–179°, in steps of 1°).

There were three main conditions in Experiment 1, performed in separate blocks. In the Low SF and High SF conditions, low or high spatial frequency Gabors were presented for the entire block of trials. In the Mixed SF condition, the two types of stimuli were randomly intermixed. The order of the three blocks was balanced across participants.

In Experiment 2 (Fig. 1C), we presented symmetric patterns of dots (Sym Dots) instead of the high spatial frequency Gabor. Sym Dots stimuli consisted of a symmetric pattern of 18 light grey dots (0.2° of diameter) created starting from a grid of 1.64 × 3.75°. The grid was divided into 8 × 8 equally sized squares, and the centre of each square was used as the dot location. Dot locations were determined with the following rule: two randomly selected columns of the 8 × 8 grid of squares contained 3 dots, while the remaining contained only 2 dots. A small jitter (0–0.015° in the x-axis; 0–0.05° in the y-axis) was added to the location of each dot. Symmetry was obtained by adding a mirrored version of the generated grid on the other side, interleaving the two specular patterns with an empty column. This empty midline represented the imaginary target orientation to be reported. Different orientations were presented by applying a rotation matrix to the entire pattern. Note that, on each trial the dot pattern was regenerated resulting in a sequential presentation of stimuli defined by the same features, but with highly variable configurations (see also Wang et al., 2016). Besides the use of symmetric dot patterns instead of high-frequency Gabors, all other aspects of Experiment 2 were identical to Experiment 1.

At the beginning of each experiment, participants were provided written and verbal instructions and performed a sequence of practice trials under the supervision of the experimenter. Practice trials were not analysed but served to ensure that participants understood the task. Experiments consisted of 3 blocks of 200 trials each, for a total of 600 trials and lasted approximately 1 h.

2.2.2. Analysis

Before statistical analysis, trials containing and following absolute adjustment errors larger than 3 standard deviations from the mean and reaction times smaller than 500 ms or larger than 10 s were removed from subsequent analyses. The first trial of each block was also removed (overall, less than 5% of trials were discarded). Adjustment errors were computed as the difference between the reported and the actual orientation in each trial, bounded to ±90°. In Experiment 1, participants performed the task with an average absolute error of 8.01 ± 1.81° and average reaction times of 1.63 ± 0.42 s. In Experiment 2, the average absolute error was 7.35 ± 1.66° and the average reaction times were 1.46 ± 0.39 s.

To quantify serial dependence, we pooled the adjustment errors of all participants (Fritsche et al., 2020) and fitted a derivative of Gaussian function (DoG) of the form:

$$error = \Delta\alpha w c e^{-(w\Delta)^2} \quad (1)$$

where Δ is the difference between the previous and current stimulus orientation, α is the amplitude of the DoG curve scaled by the constant $c = \sqrt{2}/e^{-0.5}$ to match the curve peak and w is the inverse of the curve width. The best-fitting DoG was estimated by solving a constrained nonlinear minimization problem with the sum of squared residuals as the cost function (Fritsche et al., 2020; Manassi, Liberman, Chaney, & Whitney, 2017). Constraints were imposed on both parameters to ensure algorithm convergence ($\alpha = [-20, 20]$, $w = [0.02, 0.07]$, parameters initialized at $\alpha = 2$, $w = 0.05$). DoG functions were fitted to group data, separately for each condition of interest, and the amplitude parameter α was used to quantify the bias. Statistical testing was performed using a permutation approach. A null distribution of SD amplitudes was obtained by fitting Eq. (1) to surrogate datasets generated by randomly flipping the sign of errors in each trial 10,000 times (Fritsche et al., 2020). The null distributions were used to derive p-values as the proportion of surrogate α parameters larger than the observed ones. The comparison between conditions was performed using a similar permutation approach but shuffling the labels of the conditions for each surrogate dataset.

In the analysis of the Mixed block in Experiment 1, we evaluated the qualitative predictions of two models of SD. In both models, adjustment responses were approximated by a simple adaptive filter of the form:

$$y_n = (1 - w)x_n + wx_{n-1} \quad (2)$$

where y is the adjustment response in trial n, x the stimulus orientation and w the weight assigned to the orientation in the previous trial ($n - 1$). In the ideal observer model, weights were computed as a combination of the uncertainty associated to present and past stimuli, according to the following equation:

$$w_n = \frac{\sigma_n^2}{\sigma_n^2 + \sigma_{n-1}^2 + \Delta^2} \quad (3)$$

in which σ is the uncertainty in the present (n) and past ($n - 1$) stimuli and the squared term Δ accounts for the fading of SD effects as the distance between consecutive orientations increases (Cicchini et al., 2018). The alternative model was a simplified version of Eq. (3) in which weights depended only on the uncertainty in present sensory input:

$$w_n = \frac{1}{2 + (\Delta/\sigma_n)^2} \quad (4)$$

Two σ parameters were estimated independently for Low ($\sigma = 8.21°$) and High SF Gabors ($\sigma = 4.41°$) by minimizing the difference between the peak SD predicted by Eq. (4) and the observed DoG amplitude in blocks of only Low or High SF. The two σ were then used in Eqs. (3)–(4) to predict the data in the Mixed SF block.

All model-based analyses were paralleled by a model-free approach to control that results were not affected by fitting the data to the group average (e.g., neglecting the variability at the individual level) or by model fitting artifacts. In the model-free approach, we subtracted the average error for Δ in the 1–25° range from the average error in the corresponding negative range of Δ (Samaha, Switzky, & Postle, 2019). The resulting index, quantifying the amount of systematic deviation of the errors with respect to zero (either in the positive or negative direction) was used for subsequent analysis. Effect sizes (Cohen's d') were obtained from the model-free results. The means and standard errors of the means (SEM) shown in Fig. 1-2 were computed using a moving average on the adjustment errors of individual subjects (Fritsche et al., 2017). Moving average windows were centred on the actual Δ with a length of ±7° for the data of an entire block of trials (e.g., Fig. 1A, 2A) and ± 12° for subsets of trials within the Mixed condition of both experiments (e.g., Fig. 1C, 2C), to compensate for the smaller amount of trials in Mixed blocks.

3. Results

In Experiment 1, we presented Gabors with an SF of either 0.33 or 1 cycle(s) per degree. Participants reproduced the orientation of the Gabors by adjusting the angle of an imaginary line between two response dots (Fig. 1A). Serial dependence was tested in separate blocks with Gabors having only low (Low SF), only high (High SF), or mixed spatial frequencies (Mixed SF; see Fig. 1A-B). In accordance with previous findings, in blocks with only low or high SFs, adjustment errors were positively related to the difference between the previous and

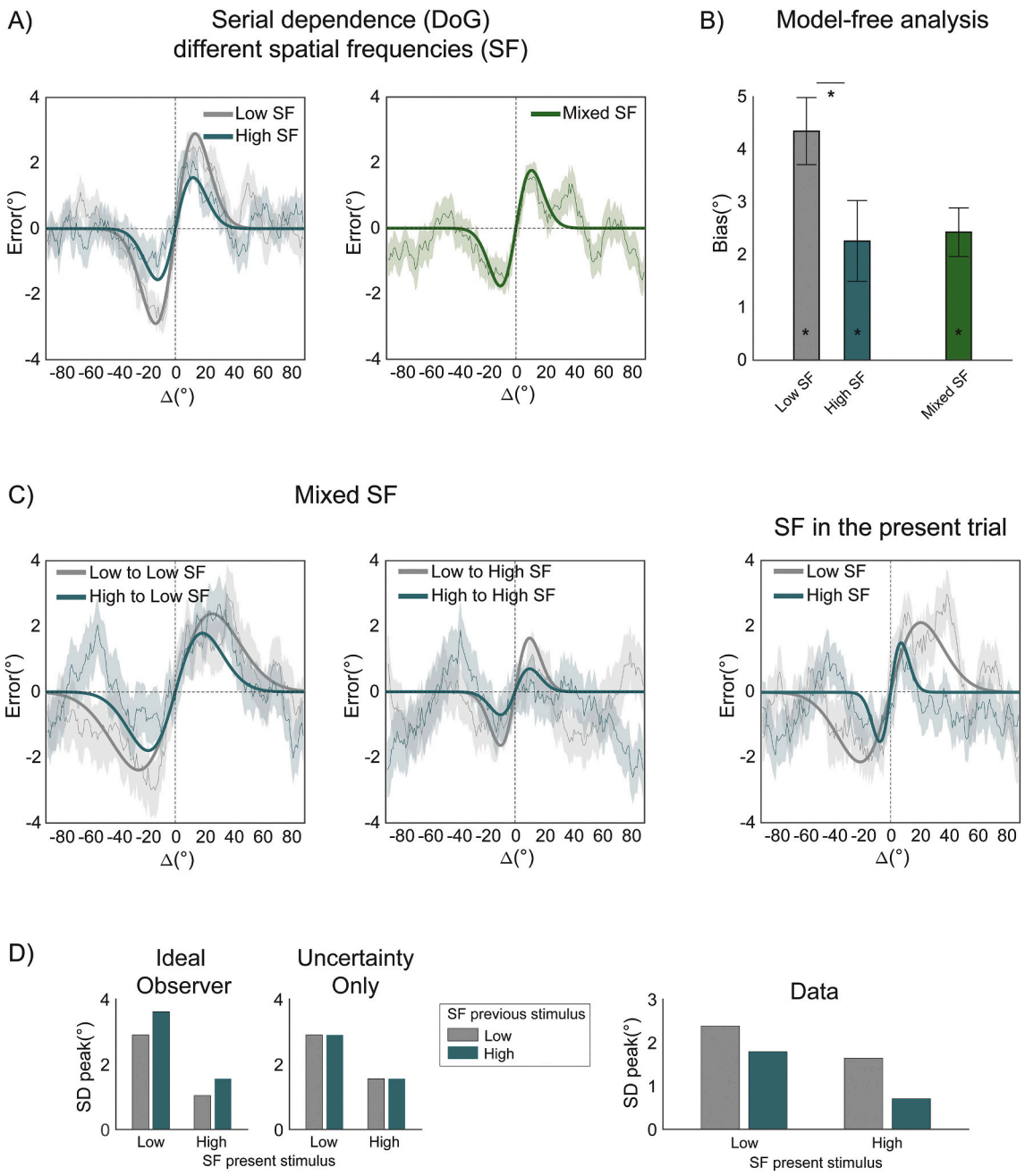

Fig. 2. A) Adjustment errors as a function of the difference between the orientation of the previous and the present Gabor (Δ), fitted by a derivative of Gaussian function (DoG). The left panel shows the adjustment errors and fits for all trials in the separate blocks with either Low or High SF Gabors. The right panel shows the results for all the trials in the Mixed SF block. Thinner lines and shaded regions represent the bootstrap estimate and standard deviation of the participants' average errors. B) Model-free analysis quantifying the SD bias as the difference between the average of errors in a positive (from 1° to 25°) and negative (from −1° to −25°) range of the Δ variable (see Methods). Error bars show the standard error of the mean (SEM). Asterisks indicate significant differences. C) SD in the Mixed SF block as a function of whether the actual trial contained a Low SF (left panel) or a High SF Gabor (central panel). The two curves in each panel indicate whether a Low or a High SF Gabor was presented in the trial before. The right panel visualizes the overall SD for Low and High SF in the actual trial of the Mixed SF block. D) Qualitative predictions of the Ideal Observer and the Uncertainty Only model, along with the observed peaks of SD amplitude in the four combinations of present and past stimuli within the Mixed SF block. The Ideal Observer model predicts larger SD when the SF of the previous stimulus is high rather than low, and the largest effect occurs in the High-to-Low SF case. The Uncertainty Only model predicts no difference due to the previous SF but an overall larger SD for Low SF Gabors. Our results (bottom bar plot) showed an opposite trend to the one predicted by the Ideal Observer model.

present Gabor orientation (Δ): more clockwise errors occurred when previous orientations were more clockwise, and the opposite was true for counter-clockwise differences (Fig. 2A). We quantified the size of this effect as the amplitude (α) of derivative of Gaussian functions (DoG) and validated this model-based analysis by an additional model-free analysis (Samaha et al., 2019; see Methods).

As shown in Fig. 2A, SD occurred in the blocks with only Low or High SF Gabors (Low SF: peak SD = 2.9°, $p < 0.001$; model-free: $t(23) = 6.83$, $p < 0.001$, $d' = 1.39$; High SF: peak SD = 1.56°, $p < 0.001$; model-free: $t(23) = 2.94$, $p = 0.007$, $d' = 0.60$). SD was larger for Low SF Gabors compared to High SF Gabors (Low vs. High: $p = 0.005$; model-free: $t(23) = 2.50$, $p = 0.02$; $d' = 0.51$, paired t-test). Importantly, SD occurred also in the mixed blocks where Low and High SF were randomly intermixed (Mixed: peak SD = 1.77°, $p < 0.001$; model-free: $t(23) = 5.26$, $p < 0.001$;

$d' = 1.07$).

In line with previous reports (Cicchini et al., 2018), SD is larger for the low spatial frequency Gabors, supposedly because they contain weaker orientation signals due to the fewer stripes. But why did SD occur in Mixed SF blocks? One possibility is that SD reflects a mechanism to reduce uncertainty in a task-relevant feature (e.g., orientation), independently of changes in other aspects of the stimulus (e.g., spatial frequency) (Cicchini et al., 2018; Kim et al., 2020). For instance, uncertainty in a sequence of orientation signals can be reduced by combining weaker stimuli (e.g., Low SF Gabors) with more reliable ones (e.g., High SF Gabors). Alternatively, SD depends on post-perceptual processes that are independent of the uncertainty of previous stimuli and affected only by the quality of current sensory input.

We illustrate these two alternatives using the predictions of two simple models of SD (Fig. 2D; see Methods). In the Ideal Observer model (Cicchini et al., 2018), sequential stimuli are combined optimally, i.e., more reliable stimuli (High SF) induce larger SD on more uncertain ones (Low SF). In a simpler alternative model (Uncertainty Only model), SD is overall larger for more uncertain stimuli (Low SF), but there is no effect of the uncertainty in the previous trial. We used these simple models to qualitatively compare their predictions against the observed patterns of SD in the Mixed SF blocks (see Supplementary Materials and Fig. S1 for a model comparison based on alternative and more sophisticated models of SD). To this aim, we estimated the peak of SD curves (DoG amplitude) separately for trials in the four combinations of the present and past SF (Low to Low, High to Low, Low to High and High to High). Qualitatively, the results provided no support for the Ideal Observer model. The SF in the previous trial had no effect on SD for both Low SF (Low-to-Low vs. High-to-Low: $p = 0.23$; model-free: $t(23) = 0.79$, $p = 0.43$) and High SF Gabors (Low-to-High vs. High-to-High: $p = 0.80$; model-free: $t(23) = 0.23$, $p = 0.81$). This pattern is consistent with the predictions of the Uncertainty Only model (Fig. 2D and S1), namely, that SD is overall larger for Low SF and unaffected by previous SF. A direct comparison of SD for Low and High SF in the Mixed block confirmed a significant increase in the width of the Low SF curve (Low SF vs. High SF, permutation $p < 0.05$), but no difference in the amplitude (permutation $p > 0.05$), in line with an overall larger bias toward previous orientations in the presence of Low SF Gabors (model-free analysis comparing errors in the $\pm 45^{\circ}$ range: $t(23) = 3.67$, $p = 0.001$, $d' = 0.75$, paired t-test; Fig. 2C, rightmost panel). We also found that, in Mixed SF blocks, SD for High SF stimuli was less pronounced compared to SD in only High SF blocks (Low-to-High SF: peak SD $= 1.6^{\circ}$, $p = 0.01$; model-free: $t(23) = 1.82$, $p = 0.08$; High-to-High SF: peak SD $= 0.70^{\circ}$, $p = 0.21$; model-free: $t(23) = 0.79$, $p = 0.43$). This suggests that participants were even less uncertain in reporting the orientation of High SF stimuli when they were intermixed with Low SF stimuli. Overall, however, the results of this experiment indicated that the two types of stimuli were not combined in an optimal way.

In Experiment 2, we tested whether SD occurs even between completely different stimuli. We used the same paradigm as in Experiment 1 but substituted the high-frequency Gabor with a pattern of symmetric dots (Sym Dots; Fig. 1C). The two stimuli appear as clearly

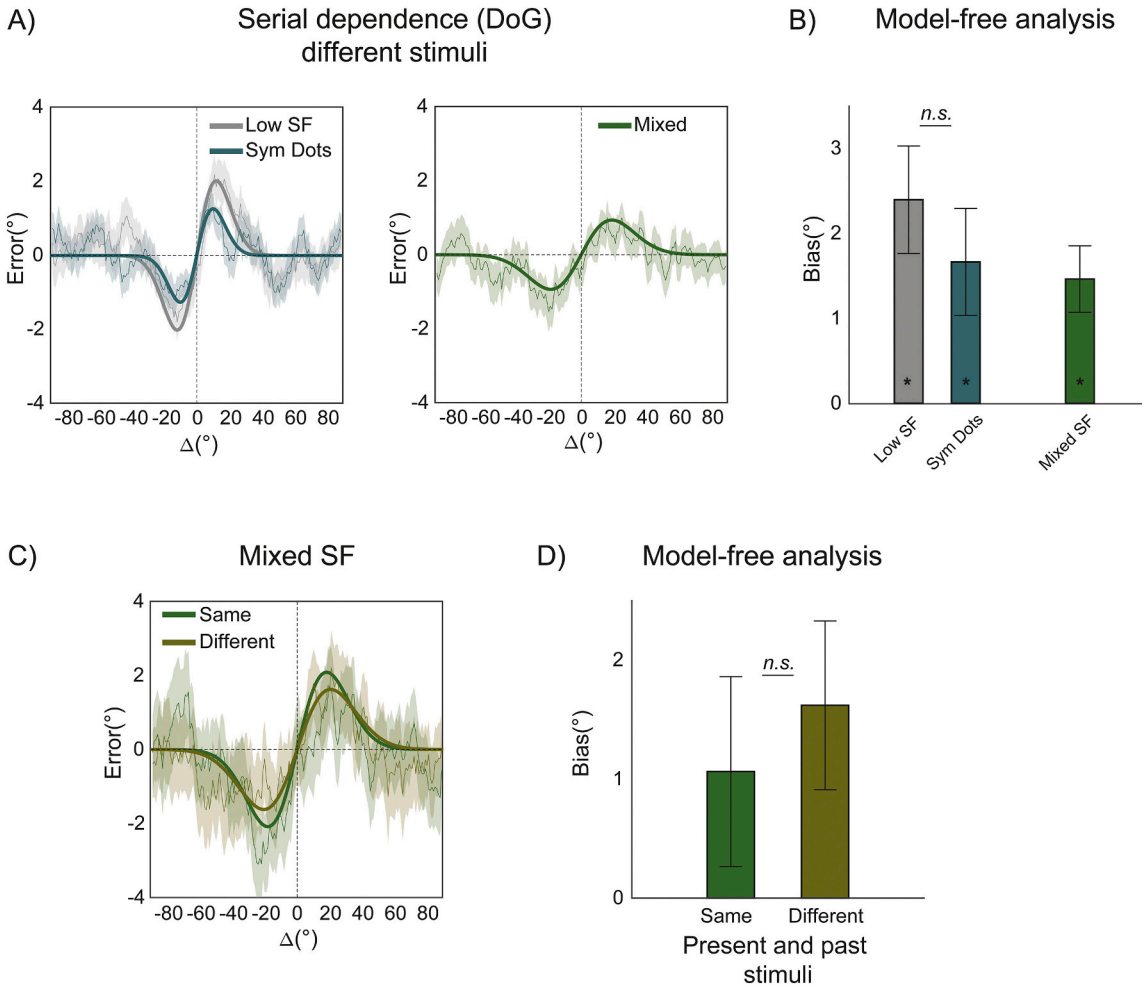

Fig. 3. A) Serial dependence and DoG fits for each block of Experiment 2. B) Model-free analysis confirming SD in all blocks, including blocks where different stimuli were intermixed (Mixed). C–D) SD in Mixed blocks was equally affected by whether the previous trial contained the same or a different stimulus.

different and are also processed at distinct stages of the perceptual stream (Wang et al., 2016), thus, SD between them would be incompatible with a purely perceptual bias. When tested in separate blocks, SD occurred for both Gabors and dot patterns (Fig. 3A-B; Low SF: peak SD = 2.02°, $p < 0.001$; model-free: $t(23) = 3.78$, $p = 0.001$, $d' = 0.77$; Sym Dots: peak SD = 1.26°, $p < 0.001$; model-free: $t(23) = 2.64$, $p = 0.015$, $d' = 0.54$), without significant difference between blocks (Low SF vs. Sym Dots: $p = 0.07$; model-free: $t(23) = 1.45$, $p = 0.16$; $d' = 0.30$, paired t-test). Crucially, SD was also present in trials of the Mixed block (Mixed: peak SD = 0.94, $p = 0.004$; model-free: $t(23) = 3.74$, $p = 0.001$, $d' = 0.76$) and was equally affected by whether the previous trial contained an identical or a different stimulus (Fig. 3C-D; same vs. different stimulus: $p = 0.33$; model-free: $t(23) = -0.44$, $p = 0.66$; $d' < 0.10$). Taken together, these results show that SD occurs for different visual features and stimuli.

4. Discussion

With two straightforward experiments, we provided evidence that the source of SD is post-perceptual. SD occurred for stimuli differing in basic features (Gabors with either Low and High SF; Experiment 1) and for entirely different stimuli (Gabor patches and dot patterns; Experiment 2). Hence, SD originates at a stage where the selectivity to specific stimulus features is lost.

Our findings have clear implications for our understanding of SD. First, previous work has often claimed that SD originates and acts at the earliest stages of visual processing (e.g., in primary visual cortex; Fischer & Whitney, 2014; John-Saaltink, Kok, Lau, & de Lange, 2016). Here we have shown that SD is incompatible with such a proposal since SD lacks the selectivity to basic visual features, which is a hallmark of early visual processing.

Second, we found that SD depends on both the decision in the previous trial and mostly on the visual quality of the present, but not on the past, stimulus (Experiment 1; Mixed SF condition). This pattern suggests that a simple Ideal Observer model is not a complete account of SD (Cicchini et al., 2018). The Ideal Observer predicts that more reliable stimuli (e.g., High SF Gabors) induce stronger SD on more uncertain ones (e.g., Low SF Gabors). This prediction was supported in a recent neuroimaging study showing that the uncertainty represented in brain activity is related to behavioural SD: more reliable sensory representations induce stronger SD on more uncertain ones (van Bergen & Jehee, 2019). However, the authors contrasted only conditions with low-to-high and high-to-low uncertainty trials. It is possible that the difference reported in their study was exclusively due to the current and not to the previous uncertainty. In the work of van Bergen and Jehee (2019), the authors also proposed a more complex ideal observer model that incorporated an internal model of the transition distribution of natural orientation changes (van Bergen & Jehee, 2019). In principle, this model can account for the lack of an effect of the previous uncertainty in our Experiment 1. For instance, if the transition distribution is broad and independent of past SF, small uncertainty differences in previous stimuli can be wiped out. It should be noted, however, that a broad transition distribution would produce comparable results to a broad decisional template that is independent of the uncertainty in past stimuli, in line with the explanation proposed here (see supplementary fig. S1).

The lack of an effect of the previous stimulus uncertainty can be alternatively explained by the fact that, in naturalistic environments, low spatial frequency stimuli tend to be more stable across time than high spatial frequency ones (van Bergen & Jehee, 2019). This may strengthen priors that increase SD after low, rather than high spatial frequency stimuli, reversing the pattern predicted by the ideal observer model. Further research may help to clarify the role of uncertainty and internal priors by using manipulations other than spatial frequency. Similarly, in evaluating the role of sensory uncertainty, we compared the predictions of the Ideal Observer model with the Uncertainty Only model. This comparison was performed using a subset of trials from one condition (Mixed SF block), leading to a reduced number of datapoints. Further research focusing exclusively on this model comparison could help to confirm and better characterize the observed patterns. Nevertheless, even if the results were qualitatively not identical to the uncertainty only model, they showed a trend opposite to the predictions of the ideal observer.

Our results, particularly those of Experiment 2, are also inconsistent with a purely Bayesian account of visual SD. Bayesian models of SD rely on the idea that our visual system uses previous stimuli as priors for present perception, exploiting the fact that stimuli in the natural world rarely change over short times (Cicchini et al., 2018; Fritsche et al., 2020; van Bergen & Jehee, 2019). In this view, the computational goal and functional role of SD is to maintain perceptual continuity and visual stability (Cicchini et al., 2018; Fischer & Whitney, 2014). This goal can be fulfilled only by a mechanism that is selective to stimulus type, i.e., combining oranges and apples has no benefit. Hence, SD for entirely different stimuli is difficult to reconcile within the framework of Bayesian perception.

We provided evidence that SD occurs beyond early perceptual processing. This may still leave open the possibility that SD involves distributed sensory areas, rather than decisional biases (Collins, 2019). SD, however, typically requires awareness (Kim et al., 2020), attention (Fritsche & de Lange, 2019) and decisions (Pascucci et al., 2019). This makes it unlikely that SD is exclusively bounded to sensory circuits and occurs without post-perceptual factors coming into play.

Whereas we conclude that the source of SD is not perceptual, we cannot rule out that SD ultimately leads to changes in the appearance of the next stimulus, i.e., that the *source* is post-perceptual but the *site of action* is perceptual (Cicchini et al., 2021). Post-perceptual decisions (Pascucci et al., 2019), as well as other recurrent processes involving higher-level areas (Kim et al., 2020), may still interfere with the decoding of orientation signals at different levels of the sensory stream, producing distortions in the appearance of both Gabors and dot stimuli. However, this late interference, which is independent of features and stimuli, suggests a common and central mechanism for SD, arguing against a continuity field in early sensory processing. A central mechanism might well explain SD in many distinct domains of processing (Liberman, Manassi, & Whitney, 2018; Liberman & Whitney, 2015) and finds support in recent evidence of SD across different stimulus features and formats (Fischer et al., 2020; Fornaciai & Park, 2019). Fischer et al. (2020), for instance, found that SD occurs after changes in task-irrelevant features but is reduced after changes in task-relevant ones (Fischer et al., 2020). Consistently with our view, this suggests that the information carried over from one trial to the next is strictly related to the task and not to the low-level properties of stimuli. Our findings also accommodate the fact that higher subjective confidence on previous reports amplifies SD independently of signal quality (Samaha et al., 2019).

In line with previous work, we propose that SD originates from post-perceptual *decisions* (Fritsche et al., 2017; Pascucci et al., 2019). This conclusion is restricted to the type of positive SD observed here and in similar studies. Other forms of SD, for example visual adaptation and negative aftereffects, are clearly of perceptual nature. Similarly, other reports showing that SD is selective for sensory modality (Fornaciai & Park, 2019) and for the ear of origin in auditory perception (Ho, Burr, Alais, & Morrone, 2019) are more difficult to frame in this view. We cannot exclude the coexistence of two sources of positive SD, one purely perceptual and the other post-perceptual (Cicchini et al., 2017), with the former fading out swiftly during inter-trial intervals and the latter dominating.

Taken together, our findings provide evidence that SD emerges at post-perceptual stages where previous events affect present reports depending on the quality of the available sensory input. The next question is, therefore, what exact mechanisms are responsible for SD. Post-perceptual accounts of SD have proposed a role for decision inertia, by which previous perceptual decisions become attractor points for

reading out and interpreting present sensory input (Pascucci et al., 2019). The fact that SD lasts only a few trials suggests the involvement of typical expectation mechanisms that emerge during sequential decisions in a random series of events. Consistently with well-known cognitive and reasoning biases, indeed, humans tend to underestimate changes in a short sequence of random events while overestimating variations over the longer term (Croson & Sundali, 2005; Pascucci, Mastropasqua, & Turatto, 2012). This perfectly fits with initial reports showing positive SD for short runs (e.g., 3–4 trials) and negative dependence for trials further in the past (Fritsche et al., 2020; Gekas, McDermott, & Mamassian, 2019).

Two recent studies have proposed a candidate mechanism for the neuronal implementation of SD that can provide a parsimonious explanation of our results. In the bump-reactivation hypothesis (Barbosa et al., 2020; Stein et al., 2020), neuronal activity from the previous trial remains imprinted in synaptic connections in the prefrontal cortex, as a latent and activity-silent pattern. Silent activity patterns are then reactivated by external cues signaling the beginning of a new trial (e.g., a fixation cue), ultimately causing serial biases in working memory. As the last representation that is held in memory most likely corresponds to the task-relevant decision, which is abstracted from low-level features, this model can perfectly explain the SD between stimuli differing in low-level aspects.

Our findings open a new avenue into the post-perceptual processes involved in SD. Post-perceptual processes can include inertia in decision-making (Pascucci et al., 2019), as well as the tendency to reiterate the same stimulus-response mapping rule (Hommel, 2004), choice repetition (Akaishi, Umeda, Nagase, & Sakai, 2014) and working-memory biases (Fritsche et al., 2017). Interestingly, it has been shown that when a different response tool is used for stimuli of different categories (e.g., response images are faces of the same or different gender as the target stimulus in a facial expression adjustment task), SD effects can be selective to the category of the preceding stimulus (Liberman et al., 2018). This suggests a role for how decisions are mapped into specific response tools that may be an important aspect for future research.

In conclusion, our results provide clear evidence that SD is not a perceptual effect but involves later processing stages where the selectivity to features and stimuli is lost.

Credit author statement

Conceptualization: DP, GC, MH. Data curation: GC, DP. Formal analysis: GC, DP. Funding acquisition: DP. Investigation: GC. Methodology: GC, DP. Project administration: DP. Resources: MH. Software: GC, DP. Supervision: DP. Validation: GC, DP. Visualization: GC, DP. Writing – original draft: DP. Writing – review & editing: GC, MH.

Acknowledgments

This research was supported by funding from the Swiss National Science Foundation (grant no. PZ00P1_179988 to DP). The funders had no role in the study design, data collection and analysis.

Appendix A. Supplementary data

Supplementary data to this article can be found online at https://doi.org/10.1016/j.cognition.2021.104709.

References

Akaishi, R., Umeda, K., Nagase, A., & Sakai, K. (2014). Autonomous mechanism of internal choice estimate underlies decision inertia. *Neuron, 81*(1), 195–206.

Bach, M. (1996). The Freiburg Visual Acuity Test-automatic measurement of visual acuity. *Optometry and Vision Science, 73*(1), 49–53.

Barbosa, J., Stein, H., Martinez, R. L., Galan-Gadea, A., Li, S., Dalmau, J., … Compte, A. (2020). Interplay between persistent activity and activity-silent dynamics in the prefrontal cortex underlies serial biases in working memory. *Nature Neuroscience, 23*(8), 1016–1024. https://doi.org/10.1038/s41593-020-0644-4.

van Bergen, R. S., & Jehee, J. F. (2019). Probabilistic representation in human visual cortex reflects uncertainty in serial decisions. *Journal of Neuroscience, 39*(41), 8164–8176.

Bertamini, M., Silvanto, J., Norcia, A. M., Makin, A. D. J., & Wagemans, J. (2018). The neural basis of visual symmetry and its role in mid- and high-level visual processing. *Annals of the New York Academy of Sciences, 1426*(1), 111–126. https://doi.org/10.1111/nyas.13667.

Bliss, D. P., Sun, J. J., & D'Esposito, M. (2017). Serial dependence is absent at the time of perception but increases in visual working memory. *Scientific Reports, 7*(1), 14739.

Brainard, D. H. (1997). The psychophysics toolbox. *Spatial Vision, 10*, 433–436.

Cicchini, G. M., Benedetto, A., & Burr, D. C. (2021). Perceptual history propagates down to early levels of sensory analysis. *Current Biology, 31*(6), 1245–1250.e2. https://doi.org/10.1016/j.cub.2020.12.004.

Cicchini, G. M., Mikellidou, K., & Burr, D. (2017). Serial dependencies act directly on perception. *Journal of Vision, 17*(14), 6. https://doi.org/10.1167/17.14.6.

Cicchini, G. M., Mikellidou, K., & Burr, D. (2018). The functional role of serial dependence. *Proceedings of the Royal Society B, 285*(1890), 20181722.

Collins, T. (2019). The perceptual continuity field is retinotopic. *Scientific Reports, 9*(1), 1–6. https://doi.org/10.1038/s41598-019-55134-6.

Croson, R., & Sundali, J. (2005). The gambler's fallacy and the hot hand: Empirical data from casinos. *Journal of Risk and Uncertainty, 30*(3), 195–209.

Fischer, C., Czoschke, S., Peters, B., Rahm, B., Kaiser, J., & Bledowski, C. (2020). Context information supports serial dependence of multiple visual objects across memory episodes. *Nature Communications, 11*(1), 1–11. https://doi.org/10.1038/s41467-020-15874-w.

Fischer, J., & Whitney, D. (2014). Serial dependence in visual perception. *Nature Neuroscience, 17*(5), 738–743.

Fornaciai, M., & Park, J. (2019). Serial dependence generalizes across different stimulus formats, but not different sensory modalities. *Vision Research, 160*, 108–115.

Fritsche, M., & de Lange, F. P. (2019). The role of feature-based attention in visual serial dependence. *Journal of Vision, 19*(13), 21.

Fritsche, M., Mostert, P., & de Lange, F. P. (2017). Opposite effects of recent history on perception and decision. *Current Biology, 27*(4), 590–595.

Fritsche, M., Spaak, E., & de Lange, F. P. (2020). A Bayesian and efficient observer model explains concurrent attractive and repulsive history biases in visual perception. *Elife, 9*, Article e55389.

Gekas, N., McDermott, K. C., & Mamassian, P. (2019). Disambiguating serial effects of multiple timescales. *Journal of Vision, 19*(6), 24.

Georgeson, M. A. (1973). Spatial frequency selectivity of a visual tilt illusion. *Nature, 245*(5419), 43–45.

Gibson, J. J. (1937). Adaptation with negative after-effect. *Psychological Review, 44*(3), 222.

Ho, H. T., Burr, D. C., Alais, D., & Morrone, M. C. (2019). Auditory perceptual history is propagated through alpha oscillations. *Current Biology, 29*(24). https://doi.org/10.1016/j.cub.2019.10.041, 4208-4217.e3.

Hommel, B. (2004). Event files: Feature binding in and across perception and action. *Trends in Cognitive Sciences, 8*(11), 494–500. https://doi.org/10.1016/j.tics.2004.08.007.

John-Saaltink, E. S., Kok, P., Lau, H. C., & de Lange, F. P. (2016). Serial dependence in perceptual decisions is reflected in activity patterns in primary visual cortex. *Journal of Neuroscience, 36*(23), 6186–6192.

Kim, S., Burr, D., Cicchini, G. M., & Alais, D. (2020). Serial dependence in perception requires conscious awareness. *Current Biology, 30*(6), R257–R258.

Liberman, A., Manassi, M., & Whitney, D. (2018). Serial dependence promotes the stability of perceived emotional expression depending on face similarity. *Attention, Perception, & Psychophysics*, 1–13.

Liberman, A., & Whitney, D. (2015). The serial dependence of perceived emotional expression. *Journal of Vision, 15*(12), 929.

Manassi, M., Liberman, A., Chaney, W., & Whitney, D. (2017). The perceived stability of scenes: Serial dependence in ensemble representations. *Scientific Reports, 7*(1), 1971.

Manassi, M., Liberman, A., Kosovicheva, A., Zhang, K., & Whitney, D. (2018). Serial dependence in position occurs at the time of perception. *Psychonomic Bulletin & Review*, 1–9.

Pascucci, D., Mancuso, G., Santandrea, E., Della Libera, C., Plomp, G., & Chelazzi, L. (2019). Laws of concatenated perception: Vision goes for novelty, decisions for perseverance. *PLoS Biology, 17*(3), Article e3000144.

Pascucci, D., Mastropasqua, T., & Turatto, M. (2012). Permeability of priming of pop out to expectations. *Journal of Vision, 12*(10), 21.

Samaha, J., Switzky, M., & Postle, B. R. (2019). Confidence boosts serial dependence in orientation estimation. *Journal of Vision, 19*(4), 25.

Sasaki, Y., Vanduffel, W., Knutsen, T., Tyler, C., & Tootell, R. (2005). Symmetry activates extrastriate visual cortex in human and nonhuman primates. *Proceedings of the National Academy of Sciences of the United States of America, 102*(8), 3159–3163. https://doi.org/10.1073/pnas.0500319102.

Stein, H., Barbosa, J., Rosa-Justicia, M., Prades, L., Morató, A., Galan-Gadea, A., Ariño, H., Martinez-Hernandez, E., Castro-Fornieles, J., Dalmau, J., & Compte, A. (2020). Reduced serial dependence suggests deficits in synaptic potentiation in anti-NMDAR encephalitis and schizophrenia. *Nature Communications, 11*(1), 4250. https://doi.org/10.1038/s41467-020-18033-3.

Wang, R., Wang, J., Zhang, J.-Y., Xie, X.-Y., Yang, Y.-X., Luo, S.-H., … Li, W. (2016). Perceptual learning at a conceptual level. *Journal of Neuroscience, 36*(7), 2238–2246. https://doi.org/10.1523/JNEUROSCI.2732-15.2016.

Ware, C., & Mitchell, D. E. (1974). The spatial selectivity of the tilt aftereffect. *Vision Research, 14*(8), 735–737.